Received: 2 February 2021 | Revised: 9 April 2021 | Accepted: 2 June 2021

DOI: 10.1002/suco.202100070

TECHNICAL PAPER

fib WILEY

Flexural behavior of slender long-span precast prestressed high-strength concrete girders

Paulo Fernandes[1,2] | **Eduardo Cavaco**[2,3] | **Paulo Maranha**[4] | **Eduardo Júlio**[2,5]

[1]Departamento de Engenharia Civil, Escola Superior de Tecnologia e Gestão, Instituto Politécnico de Leiria, Leiria, Portugal

[2]CERIS: Civil Engineering Research and Innovation for Sustainability, Portugal

[3]Departamento de Engenharia Civil, Faculdade de Ciências e Tecnologia, Universidade NOVA de Lisboa, Lisboa, Portugal

[4]Departamento de Engenharia Civil, Instituto Superior de Engenharia de Coimbra, Instituto Politécnico de Coimbra, Coimbra, Portugal

[5]Departamento de Engenharia Civil, Arquitectura e Georrecursos, Instituto Superior Técnico, Universidade de Lisboa, Lisboa, Portugal

Correspondence
Eduardo Cavaco, Departamento de Engenharia Civil, Faculdade de Ciências e Tecnologia, Universidade NOVA de Lisboa, Lisboa, Portugal.
Email: e.cavaco@fct.unl.pt

Abstract

The flexural behavior of slender (1/40) long-span precast high-strength concrete girders was experimentally investigated as a competing solution to steel alternatives for highway overpasses. Half-scale specimens were produced using an economical and high-strength (120 MPa) concrete mixture, non-fiber reinforced, designed only with conventional raw materials, currently available at Portuguese precast companies. Two girder specimens were subjected to quasi-static short-term loading up to structural failure in bending. Results have shown the typical behavior of conventional reinforced concrete members in bending, despite the brittle behavior of non-fiber-reinforced high strength concretes. Results also showed acceptable ductility (2.6) and the ability of the girder specimens to experience large deformation without significant softening. An analytical approach, based on plane sections and short-term stress–strain constitutive model recommended by the Eurocode 2 for concrete up to the C90/105 strength class, showed to predict accurately the behavior of girders in bending, both to ultimate and serviceability limit states, including cracking, yielding, maximum loads, and ultimate deflections.

KEYWORDS

bridges, girders, high-strength concrete, long-span, precast, prestressed, slender

1 | INTRODUCTION

1.1 | Motivation

In the 1990s and 2000s, Portugal made significant investments on its highway network, expanding it from just circa 300 km to more than 2700 km. In the last decade, the network was expanded only 300 km more, since most important investments are recently being directed to the widening of existing highways with significant volumes of traffic. Considering the needs of new overpasses, together with the social and economic impact of restricting the operation of these highways, this has represented a very significant market opportunity for the national precast concrete industry and an incentive to invest in research and innovation. The authors have identified the chance to develop new precast prestressed long-span girders, using high-performance concrete, and taking advantage of the improvements observed in concrete technology in the last decades, in particular (i) the production of Portland cement CEM I 52.5 R; (ii) the development of third generation super-plasticizers; and (iii) the commercialization of additions with high pozzolanic properties. They have proposed this idea of developing new precast prestressed long-span girders, capable to compete with steel alternatives

Discussion on this paper must be submitted within two months of the print publication. The discussion will then be published in print, along with the authors' closure, if any, approximately nine months after the print publication.

from both economical and structural points of view, and presented it to Prégaia, a Portuguese precast concrete company, which agreed in funding a project to make the proof of concept and build and test four prototypes. Two of these (V1 and V2) were subjected to short-term loading up to structural failure, and the remaining two were reserved to study the long-term time-dependent structural behavior. This paper presents the major findings related to the test of specimens V1 and V2.

1.2 | Background

In the last decades, significant research has been devoted to the study of high-performance concrete (HPC) and, more recently, to ultra-high-performance concretes (UHPC), either fiber-reinforced (UHPFRC), or not.[1–6] The most significant research on the use of UHPC for practical applications on infrastructures, namely for bridge girders, has been conducted by the Federal Highway Administration (FHWA) of the U.S. Department of Transportation. In fact, the first studies considering the use of precast prestressed long-span girders using HPC on bridges were carried out by the Louisiana and Texas states transportation departments[7–11] in the 1990s and 2000s. From these pioneer studies, the advantages of using this material on bridge girders became evident since their use allows a design with longer spans, fewer and increased spacing between girders, and improved durability. The major drawback is the brittle behavior usually related with high strength concretes. In the last decade, and taking advantage of the advances on the concrete technology and the development of UHPFRC, the FHWA kept investigating toward their use on bridges.[12]

In spite of the above-mentioned, the majority of the research on UHPC and UHPFRC has addressed chemical, mechanical, and physical properties of the material itself, whereas the research on its practical application is still scarce. For instance, on bridge girders, pre-mixed fiber-reinforced proprietary mixtures have been used for a long time. As a result, their cost is significantly high, being this the major reason for their marginal use. Lastly, it should be highlighted that testing of real scale specimens is almost inexistent in the published research.[5,6]

1.3 | Research significance

Fast and efficient widening of highways' cross-section demands structural solutions with reduced height/span ratio to avoid the reduction of its gabarit and/or changes on the profile of the road above. Since current prestressed concrete girders available at the precast Portuguese market show a height/span ratio above 1/30, steel girders are the preferred structural solution.

The main goal of the project herein described was to develop prestressed concrete girders that could represent an economical alternative to steel girders on the construction of long-span highway overpasses. In addition, and since significant investments are expected to be dedicated to the cross-section widening of several highways, the prestressed concrete girders to be developed should exhibit slenderness similar to that of the competing steel girders, due to minimum gabarit requirements, and costs of changing the profile of the road above. In particular, and considering the cross-section widening from 2×2 to 2×3 carriageways, the prestressed elements aimed to be produced should have a span of 40 m and a height/span ratio of 1/40, which corresponds approximately to a reduction of one third in slenderness, in comparison to most widely used prestressed concrete girders (1/30). Having in mind the economic competitiveness of the structural solution, it should be highlighted that, in order to be cost-effective, the concrete mixture for the bridge girders should be reliably and consistently produced and designed using current constituents, that is, those available at typical industrial plant, such as the one where the prototypes were going to be produced.

To achieve the described ambitious goal, it was considered to be crucial to reach high mechanical properties to significantly reduce the cross-section of the beams and, thus, to reduce both the production costs and the beams' deadweight, the latter also leading to a reduction in transportation costs, as well as to an increase in the productivity of the company, due to the high compressive strength obtained at early ages, allowing much shorter curing times. Thus, and based on the expected traffic loads, the span, and the height/span ratio, a compressive strength of circa 120 MPa was defined as target, which corresponds approximately to the highest concrete strength class (C90/105), according to Eurocode 2,[13] that is, the code adopted in the European zone. According to the American Portland Cement Association, this is the minimum strength for a classification as a UHPC. However, UHPCs are usually fiber reinforced and coarse aggregates free. At this point, it must be stressed out that, in this case, always considering the economic perspective, only raw materials already available at the precast plant were adopted. Therefore, the first part of the project was entirely dedicated at designing the concrete reference mixture, using only constituents available at the industrial plant, including the mechanical characterization of the adopted UHPC in the hardened state.[14] The present paper addresses the experimental characterization of the structural behavior of half-scale specimens tested in bending up to failure.

2 | MATERIALS AND METHODS

The main goal of the project was to produce economic and competitive precast prestressed high-performance concrete girders for highway overpasses with a height/span ratio of 1/40, thus capable to cross a 2 × 3 carriageways profile (40 m) with a maximum deck depth of 1 m. The main constraint of the production process was the mandatory use of only current raw materials available at the Prégaia precast plant.

The experimental work herein described aims at studying the structural behavior and ductility of the produced specimens, in particular; (i) the bending strength; (ii) the failure modes and ductility; and (iii) the accuracy of the design expressions, recommended by Eurocode 2,[13] to predict the specimen's behavior under ultimate and serviceability conditions.

Four I-girder specimens (V1–V4) were produced at the Prégaia industrial plant (see Figure 1). The first two, V1 and V2, were used and tested in this study. The remaining two were left for further investigation regarding the time-dependent effects. Due to laboratory space constraints, half-scale specimens were produced, that is, with 20 m length and a cross section depth of 0.50 m, corresponding to 1/40 depth to span ratio (see Figure 2). Web thickness was defined equal to 75 mm to allow adequate flow of the concrete mixture. Flange's width was set equal to 0.30 m with a minimum thickness of 75 and 60 mm, for the bottom and top flanges, respectively, due to the size of the prestressing strands and magnitude of the applied prestressing stresses (30 MPa). Figure 2 shows the reinforcement detailing of the specimens. For the longitudinal passive reinforcement, as well as stirrups, S500ER steel grade reinforcing bars with 5 mm diameter were used. Strands of a low-relaxation steel grade Y1860S, each one with seven wires, with 9.3 mm (3/8″) diameter, were used for prestressing the specimens. Considering the depth to span ratio and the reinforcement detailing, failure of the specimens was predicted in bending when subjected to a four-point loading test.

As previously referred to, the mixtures' design is published in the study by Fernandes et al.[14] For the current study, an economic concrete mix with mean compressive strength of circa 120 MPa and high workability (S5 class according to European Committee for Standardization[15]) was adopted. The corresponding constituents and proportions are presented in Table 1. The assessment of the compressive strength was carried out according to European Committee for Standardization[16] using three 15-cm cubic specimens per girder specimen. Tests were performed at 28 days, at the prestress transference day, and at the day of testing. Results are presented in Figure 3 and Table 2. A

FIGURE 1 Cross-section of the I-girder specimens

tendency law was derived, given by Equation (1), and presenting a coefficient of correlation equal to $R^2 = 99.97\%$.

$$f_{cm}(t) = \frac{t}{0.0076t + 0.0319} \quad (1)$$

For the Young's modulus, two prismatic specimens with 15 cm × 15 cm × 600 cm were used. Tests were performed at 7th, 28th, 112th, and 224th days. Results of the mean values are presented in Table 2 and Figure 4. Equation (2) provides a tendency line with a coefficient of correlation equal to $R^2 = 99.99\%$.

$$E_{cm}(t) = \frac{t}{0.0165t + 0.0197} \quad (2)$$

To assess the prestressing losses due to creep and shrinkage of concrete up to the testing day, four prismatic specimens with 15 cm × 15 cm × 600 cm were produced. The first two cured close to girder specimens, thus under identical hygrothermical conditions. The remaining two were placed in the same environment and loaded under a constant stress of 30 MPa. A hybrid oil and gas actuated press was used to keep the stress level accurately constant on the long term. Strains due to shrinkage were evaluated using unloaded specimens, and by measuring the relative displacements between two cross sections distanced 30 cm apart at several different ages, using a linear transducer with a precision of 1 μm. Identical measurements were made on loaded specimens at the same ages. Creep was obtained by subtracting strains due to the elastic deformation (measured in loaded specimens) and shrinkage (measured in unloaded specimens) from the global strain (measured in loaded specimens). Finally, the creeping coefficient was calculated considering the Young's modulus at 28 days of age. Table 3 summarizes measurements of creep and shrinkage at the closest dates to the testing day of

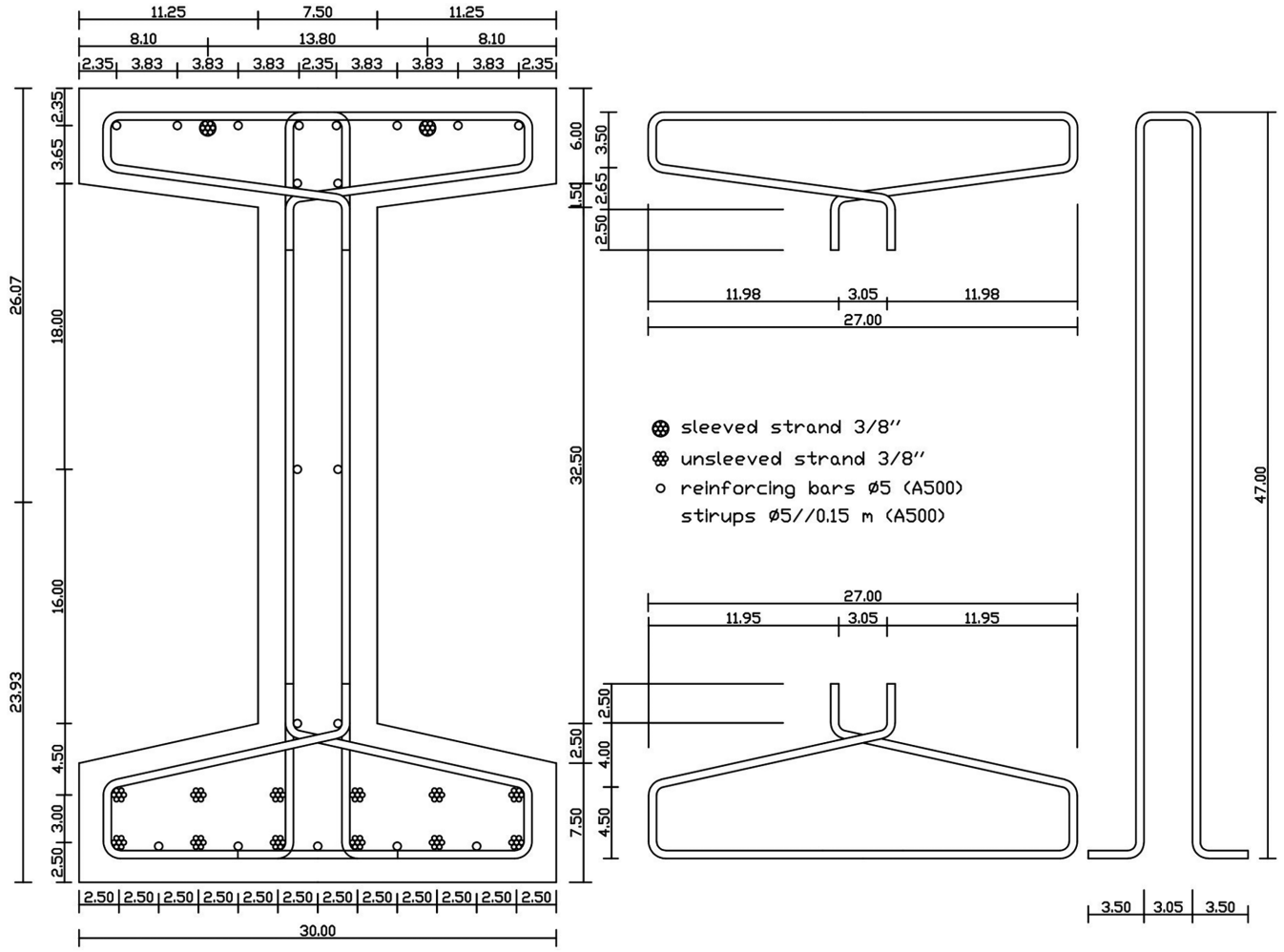

FIGURE 2 Reinforcements of the I-girder specimens

TABLE 1 Concrete mixture proportions (adapted from[14])

Constituent	Designation	Quantity/m^3
Cement (C)	CEM I 52.5R	500 kg
Addition (Ad)	Sikacrete HD	50 kg
Coarse Aggregate (CAg)	Granite gravel	532 kg
Fine Aggregate (FAg)	River sand	1167 kg
Admixture (Adm)	Sika ViscoCrete 20 HE	10.2 L
Water (W)	—	144.0 L

specimens V1 and V2. A linear interpolation was used to estimate their values at these days.

Six samples of both the passive reinforcing bars and the active strands were subjected to tensile tests according to EN 10080.[17] Results of the mean values of the yielding stress and ultimate stress and strain are presented in Table 4. The 12 strands at the bottom flange were prestressed up to 72% of the material's ultimate strength (1430 MPa). These were left in direct contact with concrete to remain adherent after the prestress transfer. The two strands on the top flange were designed as non-active in situ. Their role was just to avoid decompression of the top flange after completing the prestress transfer to the bottom strands, and during the transportation to the laboratory facilities, up to the testing day. In this manner, these strands were sheathed on a PVC sleeve and left non-adherent. These were stressed up to 60% of the steel's ultimate strength (1180 MPa). Prestress transfer was completed at the 12th and 10th days, for specimens V1 and V2, respectively, firstly on top strands and finally on bottom strands. An initial precamber of approximately 26 mm was measured on both specimens.

On the laboratory facilities, specimen V1 was first submitted to a free vibration test at the 97th day to check specimen integrity, to assess the natural frequencies of vibration on vertical direction and the corresponding damping ratios. The specimen was simply supported and

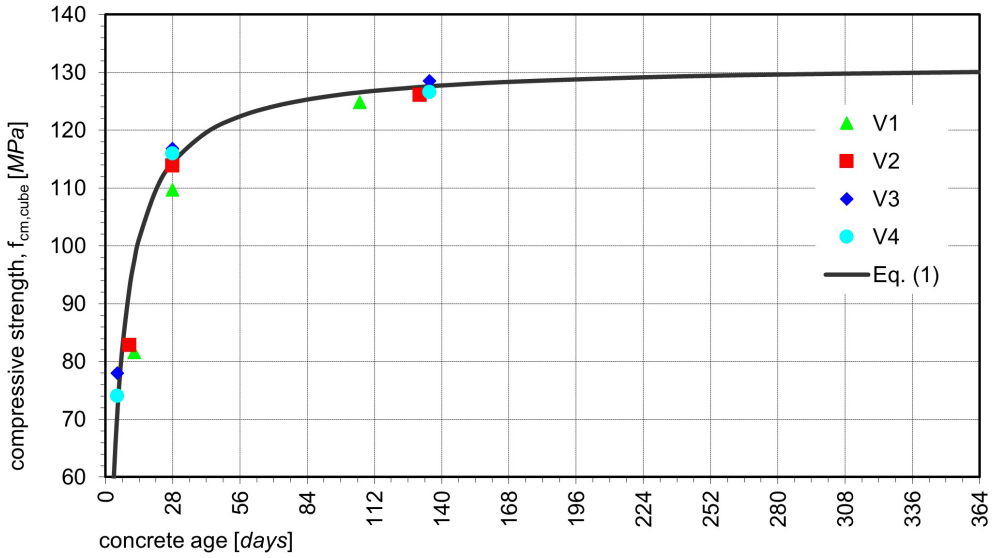

FIGURE 3 Development of compressive strength with time

Specimen	Compressive strength f_{cm} (MPa) at Prestress transference day	28 days	Testing day
V1	81.6 (12th day)	116.8	124.8 (106th day)
V2	82.8 (10th day)		126.1 (131th day)
V3 and V4	75.6 (5th day)		127.6 (135th day)[a]

Young's Modulus E(GPa) at 7 days	28 days	112 days	224 days
52.8	58.5	60.0	60.2

TABLE 2 Concrete mechanical properties

[a]Tests of specimens V3 and V4 are not presented in this paper.

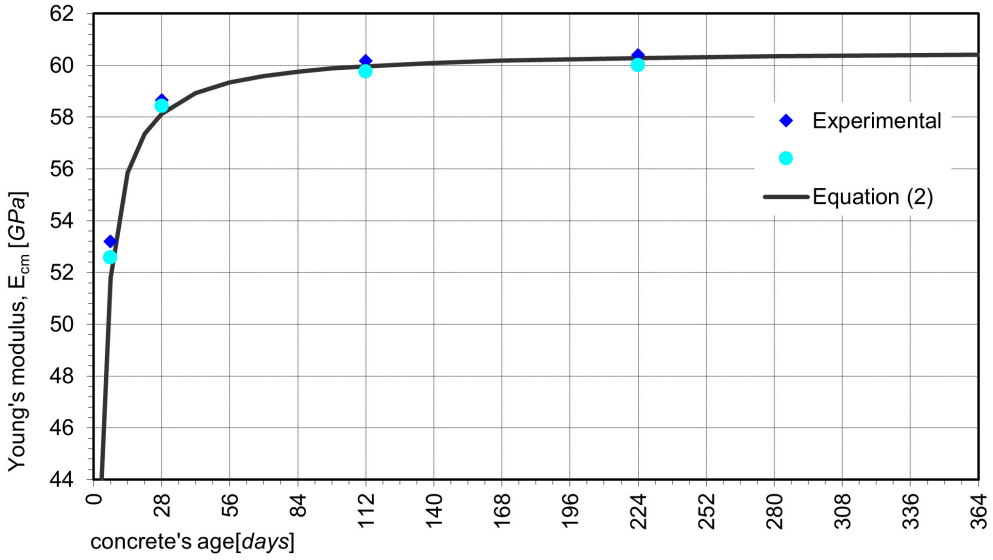

FIGURE 4 Development of the Young's modulus with time

loaded with a suspended mass at the mid-section. Considering the specimen's symmetry, half of its length was monitored with accelerometers placed at the bottom flange of seven different sections (see Figure 5a). After unloading it instantaneously, the specimen was allowed to freely vibrate for approximately 60 s. During this period, the accelerations on the sections referred to were recorded (see Figure 5b). Finally, a modal analysis was

TABLE 3 Creep and shrinkage

Strain	98th day	112th day	126th day	135th day
Global, $\varepsilon_{c(e,s,c)}$ (‰)	1.865	1.871	1.877	1.881
Elastic, ε_{ce} (‰)	0.527			
Shrinkage, ε_{cs} (‰)	0.210	0.211	0.211	0.212
Creep, ε_{cc} (‰)	1.128	1.134	1.139	1.142
Creeping Coefficient, φ_c	2.413	2.425	2.437	2.445

carried out using the "peak picking" method and the PULSE ® software from Bruel & Kjaer (see Figure 5c).

After the free vibration test, both specimens were subjected to a four-point loading test, as shown in Figure 6. The test load was applied indirectly by means of an auxiliary heavy-duty steel beam, simply supported on the girder specimens and loaded centrally (see Figure 7). This way, the applied load was transferred to two sections distanced 6.0 m apart, thus defining a central length subjected to pure cylindrical bending. The distance of these sections to the supports was 6.825 m. On these sections, Teflon side guides were used, to avoid lateral instability of specimens under large displacements (see Figure 7).

A hydraulic actuator with 1000 kN/300 mm capacity, reacting against a steel frame prestressed to the strong floor, was used to apply the test load. A load cell was coupled to the actuator to record the applied force, *P*. The auxiliary heavy-duty steel beam was connected to the strong floor with steel rods, to allow the reposition of the actuator without unloading the specimens, when its maximum displacement was reached.

At the supports' sections (S1 and S11), and at the sections of load transfer, from the steel beam to the girder specimen (S5 and S9), three load-cells per section were used to monitor the established equilibrium, two below the structural element and one above (see Figure 8). Steel plates and rods were used to connect the load cells and avoid these to fall under large displacements/rotations (see Figure 9). Linear Variable Differential Transformers (LVDT) were used at sections S2 to S10 to monitor displacements, δ_i, and set the deformed shape of tested specimens. Terrestrial photogrammetry was also used for this purpose. Photo targets were installed on the top and bottom flanges and at the middle of the web and spaced 0.50 m apart (see Figure 9). Strain gauges were attached to the bottom, top, and web of longitudinal passive reinforcement, at sections S2–S4, S6–S8, and S10. A data logger was used to record all the data provided by the monitoring devices. The experimental tests were performed under displacement control, increased at a rate of 0.2 mm/s, up to the specimen's failure.

Finally, 2-m length samples were cut in bottom flanges within the specimen length defined between sections S1 and S3, since herein, and as explained further in the paper, the specimen did not experience plastic deformations. The existing prestressing level on the adherent strands was assessed after their extraction with a jackhammer and its unstressed length was measured (see Figure 10).

3 | RESULTS AND DISCUSSION

Table 5 shows the frequencies of vibration for the first four vertical modes, obtained during the experimental free vibration test. Since these girders are expected to be used together with a top reinforced concrete slab, to serve as bridge deck, the obtained results cannot be extrapolated for real operating conditions but, nonetheless, they provide information on the specimens' stiffness and condition.

Table 5 also shows frequencies of vibrations estimated based on Equation (3), which result from the differential equation of motion of a beam, considering free and undampened vibrations. Comparison to experimental results shows a sound agreement between both. A 1.5% difference exists between the frequencies of vibration for the 1st mode. The calculation of the Young's modulus using Equation (3) and assuming the natural frequency of vibration assessed experimentally, 3.34 Hz, results in 58.6 GPa. An estimation of the Young's modulus at the free vibration test day (97th day), based on Equation (2) results in 59.9 MPa, which corresponds to a deviation of 2.2%.

$$f_n = \frac{n^2\pi}{2L^2}\sqrt{\frac{EI_h}{m}} \tag{3}$$

Results of damping ratios are also presented in Table 5. For the 1st to the 4th modes, damping range from 0.41% to 0.78%. According to Bachmann et al.,[18] this is the expected range of damping for uncracked prestressed concrete, which corresponds to pure viscous damping. From the results of the free vibration test, it is possible to conclude that the produced specimens present acceptable quality and condition.

TABLE 4 Mechanical properties of reinforcing bars and prestressing strands

Steel grade	Diameter ϕ (mm)	A_s (mm^2)	f_{ym} (MPa)	f_{um} (MPa)	ε_{um} (%)	E (GPa)
A 500 ER	5	19.6	604	646	11.5	200[a]
Y 1860 S	9.3	52.5	1815	1975	5.0	192[b]

[a]Assumed.
[b]Measured in strands.

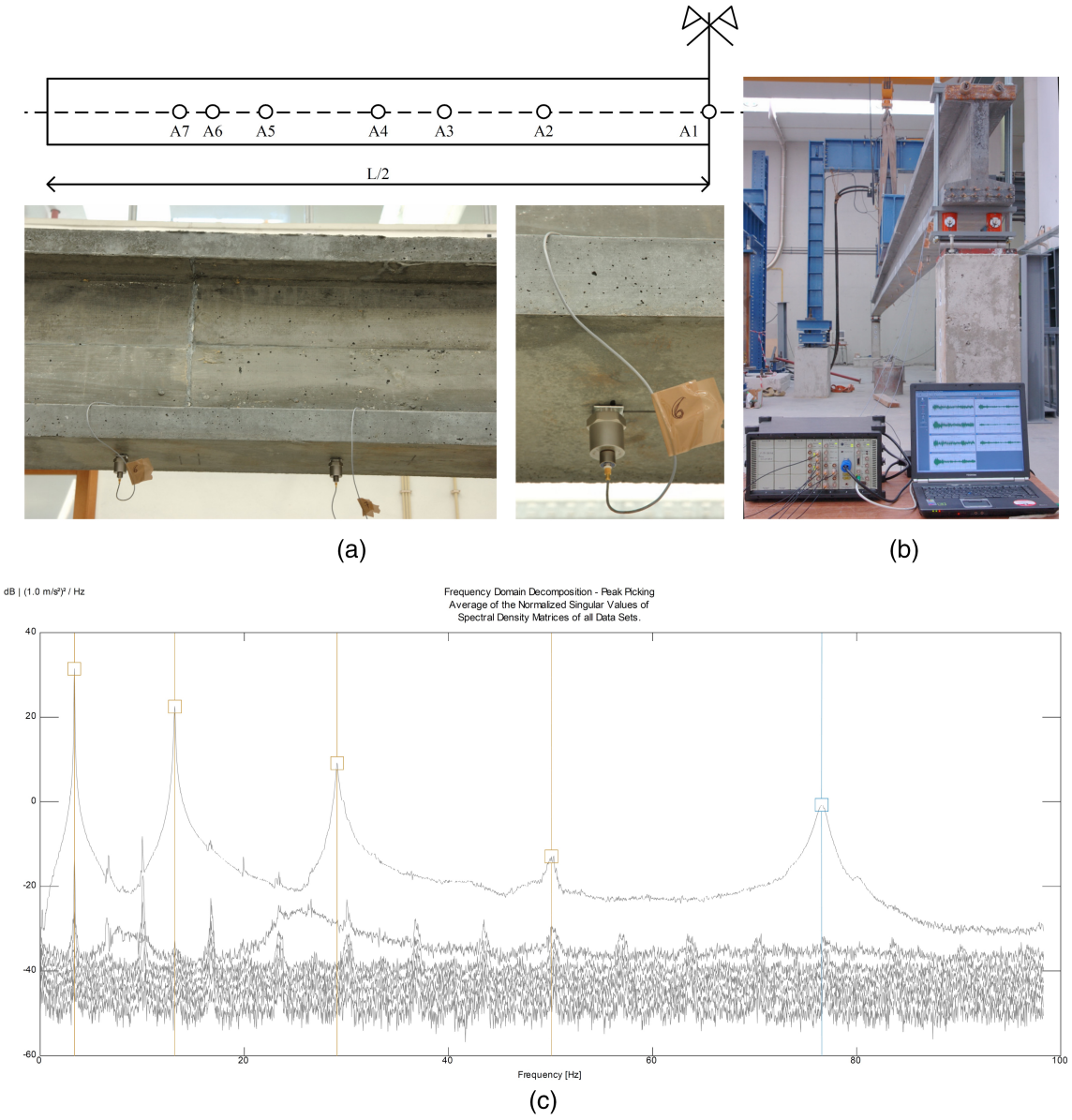

FIGURE 5 Dynamic characterization of specimen V1: (a) accelerometers on monitored sections; (b) free vibration of specimen; (c) modal identification using the "peak picking" method

Figure 11 shows the load–displacement diagrams recorded during the loading tests of girders V1 and V2. The measured displacements, δ_7, correspond to those at the midspan section (S7). It was observed that both girders exhibit similar global behavior, although girder 1 presents slightly less stiffness and strength, eventually due to a younger age of concrete at the day of testing, with a lower compressive strength (see Table 2). On both specimens' diagrams, the three typical bending behavior stages are well depicted: (i) stage I—elastic and uncracked behavior; (ii) stage II—crack spreading phase along the specimen's length, up to the yielding of the longitudinal

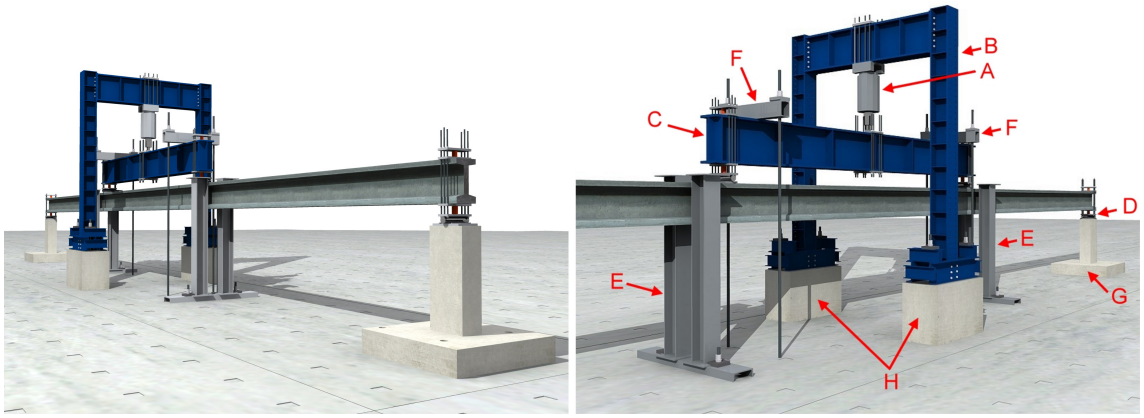

FIGURE 6 Four-point loading test setup

FIGURE 7 Testing setup

FIGURE 8 Monitored section

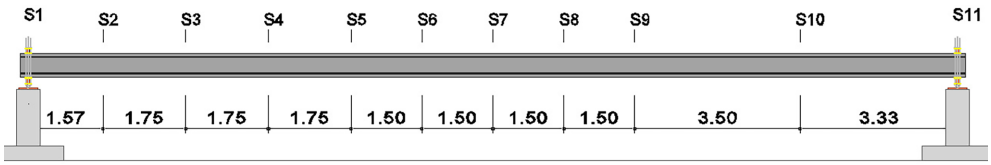

reinforcement in tension; and (iii) stage III—spread of yielding along longitudinal reinforcing bars and development of the failure mechanism. The non-linear behavior of the specimens was considered stable and adequate without relevant load drops in stage II and negligible softening along stage III (see Figures 11 and 12b). The end of the test (and end of stage III) was characterized by the sudden and abrupt failure of the specimens at the mid-span section (see Figure 12b). No post-peak behavior was observed due to the more brittle behavior of the high-grade concrete used. As depicted in Figure 12c,d, failure of the mid-span section was caused by crushing of concrete on the top flange and fracture of the longitudinal reinforcing bars. The failure section was well localized contrary to bending failures of less slender girders. Sections in the vicinity of the failure section remained undamaged, which reflects the brittleness of the concrete's grade used, compared to lower grade materials.

Extraction of tendons on the bottom flange (see Figure 10) followed by measurement of their unstressed length revealed prestress losses around 16%, on both specimens. Results of the loads corresponding to the end of both stages I and II, as well as of the maximum recorded during stage III, thus respecting to cracking (P_{cr}), yielding (P_y), and specimens' maximum load-carrying capacity (P_{max}), respectively, are presented in Table 6, for both the specimens, as well as the matching bending moments at the mid-span section. These were calculated based on the effect of: (i) the testing load; and (ii) the latter plus the effect of specimen's self-weight (90 kNm).

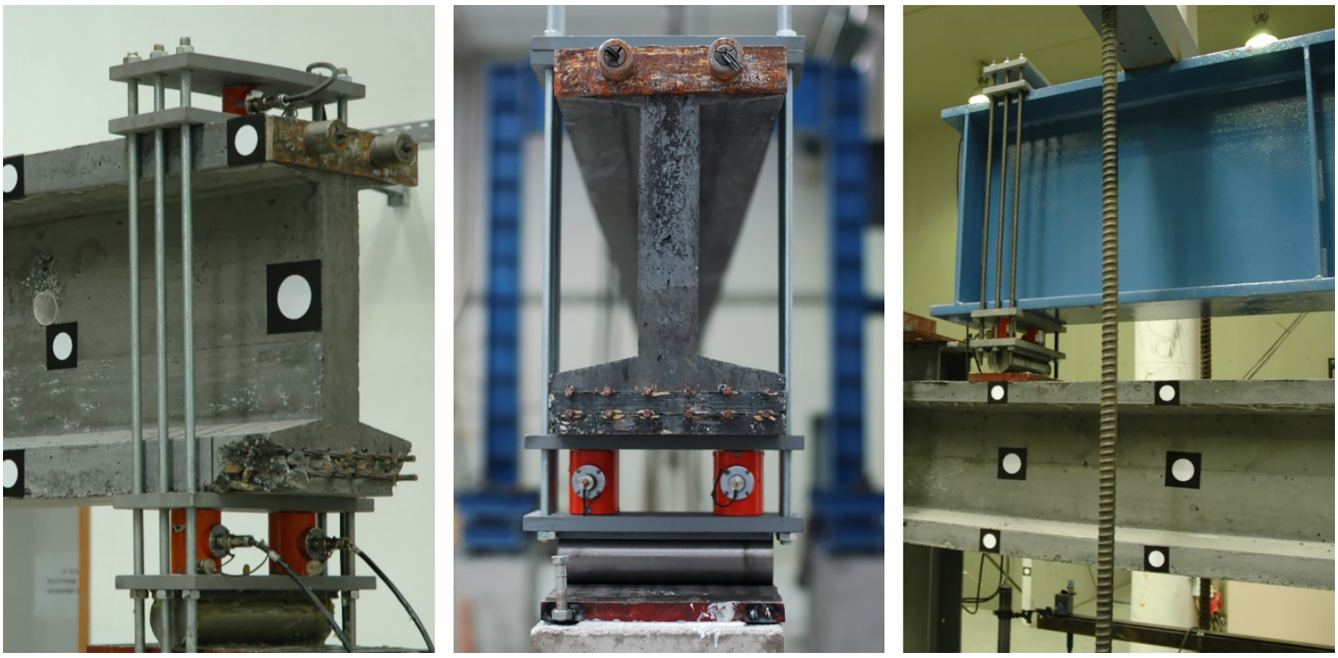

FIGURE 9 Load cells attachment at support and loading sections

Experimental cracking load, P_{cr}, was estimated based on the appearance of the first cracks during the tests, and on the observation of the end of the linear elastic branch of the load–displacement diagram presented in Figure 11. The yielding load, P_y, was considered as the one corresponding to yielding of most of the lower prestressing tendons. For that load, a strain of 3.3‰ was recorded on strain gages attached to the ordinary reinforcing bars placed at the same distance of the neutral axis. As referred to, prestress losses were roughly evaluated as 16%, following the destructive tests. Thus, the stress–strain levels on the lower tendons, at the testing day, were estimated in 1201 MPa and 6.2‰, respectively. Considering the mechanical properties of tendons presented in Table 4, it was concluded that the yielding strain (9.5‰) was reached when the strain gauges indicated readings of 3.3‰. For this purpose, records of the strain gages attached to the reinforcing bars at the mid-span section were used (see Figure 13 for specimen V1). Finally, the load-carrying capacity, P_{max}, was considered as the maximum force recorded during the entire test.

Table 6 also presents the yielding and ultimate displacements measured at the mid-span section. The ratio between the ultimate and the yielding displacement was calculated as a ductility indicator. Despite high strength concretes tend to exhibit a brittle behavior, in particular those non-fiber reinforced, this ratio resulted equal to 2.6, for both specimens, thus showing an acceptable ductility.

Estimates of most significant load values (cracking, yielding, and load-carrying capacity) were also reached based on the calculation of the corresponding bending moments at the mid-span section, considering: (i) the hypothesis of plane sections (see Figure 14); and (ii) the idealized stress–strain law for concrete, steel reinforcing bars and prestressing tendons, recommended by Eurocode 2[13] and Model Code 2010.[19]

For concrete, the non-linear stress–strain relationship for short-term loading was used, considering the compressive strength and the Young's modulus obtained experimentally at the testing day (see Table 2). For the reinforcing bars and prestressing tendons, the idealized strain-hardening bilinear model was used, considering the yielding and tensile stresses and strains obtained experimentally (see Table 4).

A *Delphi* routine was developed to calculate the resisting bending moment corresponding to the cross-section stress–strain diagram depicted in Figure 14, given the axial acting force and a strain limit, either on the top most compressed fiber, or on the reinforcing bars placed at the bottom flange. Alternatively, the routine also provided the stress/strain of any given fiber, as well as the cross-section curvature for the acting bending moment and the axial force. Calculations were performed considering the initial stress and strain installed in the materials resulting from tendons prestress, and the linear-elastic and time-dependent effects, from the production day up to the testing day, including the effect of self-weight. In

FIGURE 10 Assessing stress level on prestressing strands: (a) cutting strands; (b) exposing it; (c) measuring unstressed length

TABLE 5 Frequencies of vibration and corresponding damping ratios

Experimental results	1st mode	2nd mode	3rd mode	4th mode
Frequency (Hz)	3.34	13.19	29.09	50.07
Damping (%)	0.78	0.41	0.49	0.57
Frequency Equation (3) (Hz)	3.39	13.55	30.48	54.19

particular, the level of stresses installed on the prestressing tendons at the day of testing was assessed considering the initial pushing force and the following losses due to: (i) instantaneous deformation of the specimen; (ii) relaxation of the prestressing tendons; and (iii) concrete's creep and shrinkage. For the former losses, the Young's modulus of concrete evaluated at the prestress transfer day was used (see Table 2). Relaxation of the prestressing tendons was assessed according to Eurocode 2,[13] considering the relaxation coefficient recommended by the tendon's supplier, $\rho_{1000} = 2.5\%$. Losses due to creep and shrinkage were evaluated considering the experimental results presented in Table 3.

Since no significant differences were observed between the mechanical properties of concrete of specimens V1 and V2, and between the age dependant parameters (relaxation, creep, and shrinkage), a single estimation of the prestressing losses was performed, considering, for the controlling parameters, mean values between the two specimens. In this case, the total losses of prestress up to the testing day were estimated in 16.1% and 10.4%, for the adherent and the non-adherent tendons, respectively, which correspond to tensile stresses of 1200 and 1050 MPa,

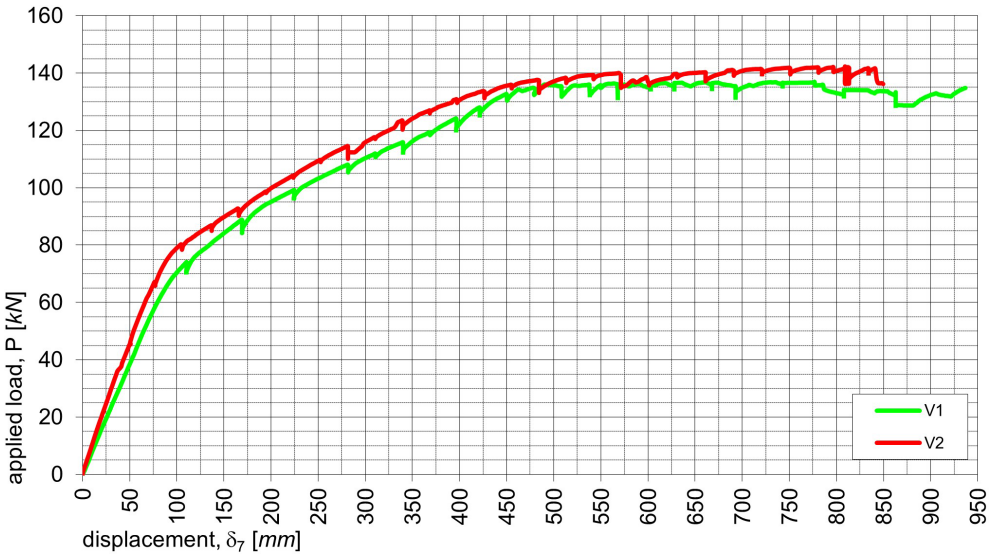

FIGURE 11 Load–displacement diagrams of specimens V1 and V2

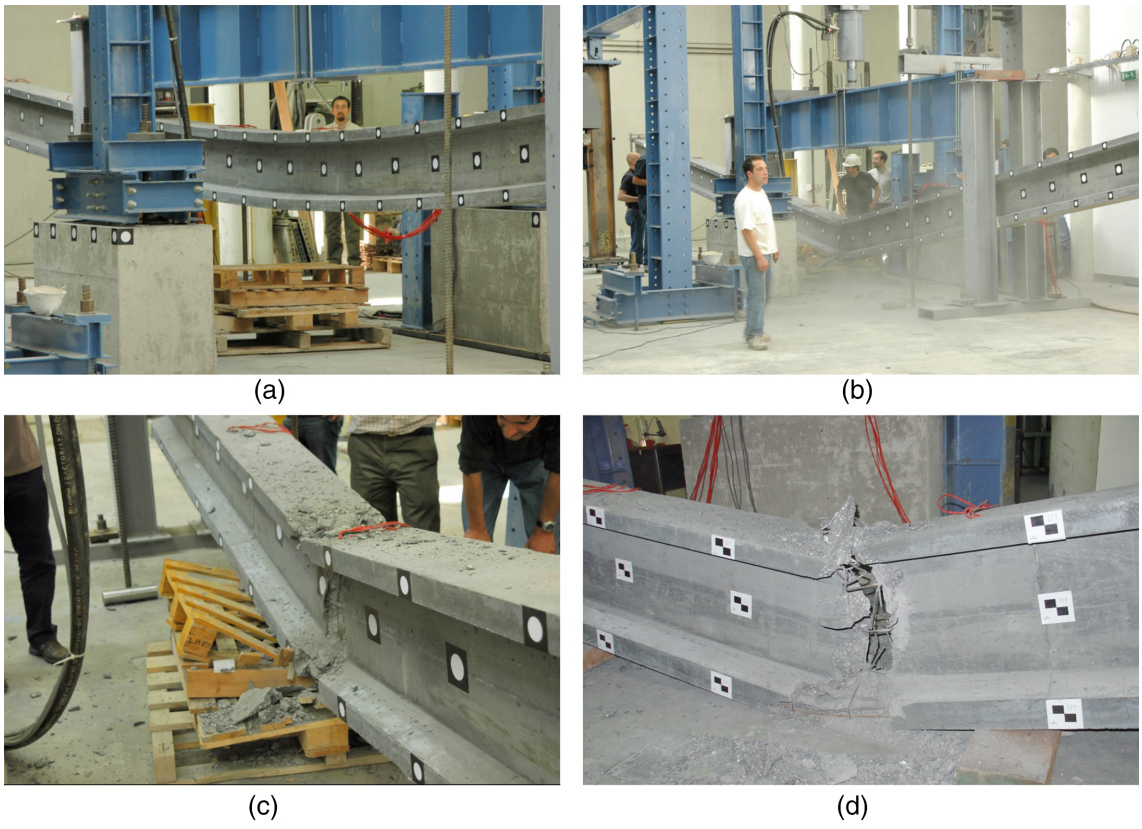

FIGURE 12 Loading test of specimen V2: (a) stage III (b) collapse; (c) and (d) crushing of concrete and fracture of reinforcing bars at the mid-span section

respectively. The former agreeing with the results of the destructive tests (16%).

Analytical estimates of the loads/bending moments corresponding to cracking, P_{cr}/M_{cr}, yielding, P_y/M_y, and load-carrying capacity, P_{max}/M_{max}, of the tested specimens, presented in Table 6, exhibit negligible differences when compared to experimental results. The maximum relative difference was 10% for the cracking load of specimen V2. Maximum relative difference between load-carrying capacity of specimens was 2.5%, achieved for specimen V1.

The obtained results presented in Table 6 show that Eurocode 2[13] designs assumptions, regarding concrete's

TABLE 6 Summary of the experimental tests and analytical results

Specimen	Experimental				Analytical		
	P_{cr}/M_{cr} (kN/kNm)	P_y/M_y (kN/kNm)	P_{max}/M_{max} (kN/kNm)	δ_y/δ_u (mm/mm)	P_{cr}/M_{cr} (kN/kNm)	P_y/M_y (kN/kNm)	P_{max}/M_{max} (kN/kNm)
V1	60/295	118/493	137/558	365/936	60/296	123/510	141/572
V2	66/315	120/500	142/574	331/850			

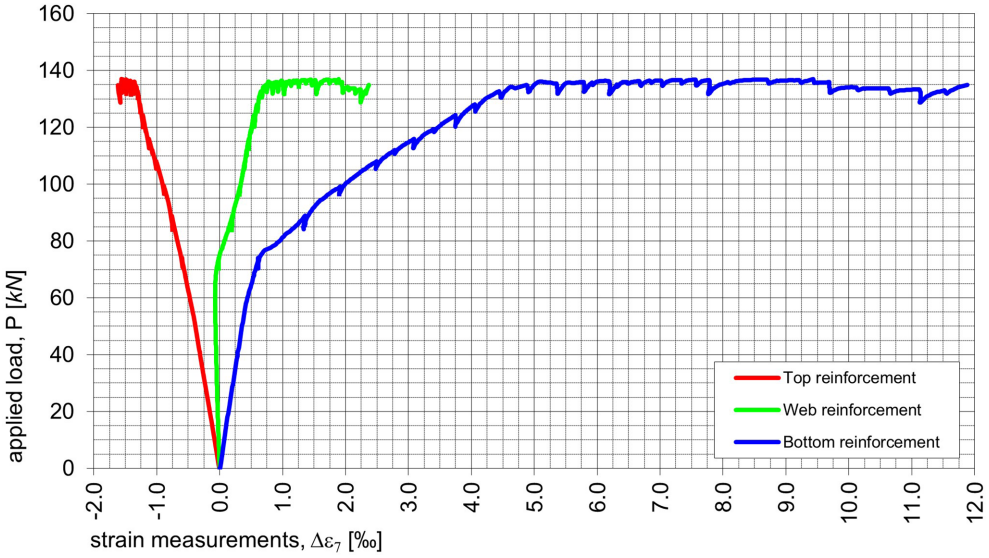

FIGURE 13 Strain gauges records on section S7 of specimen V1

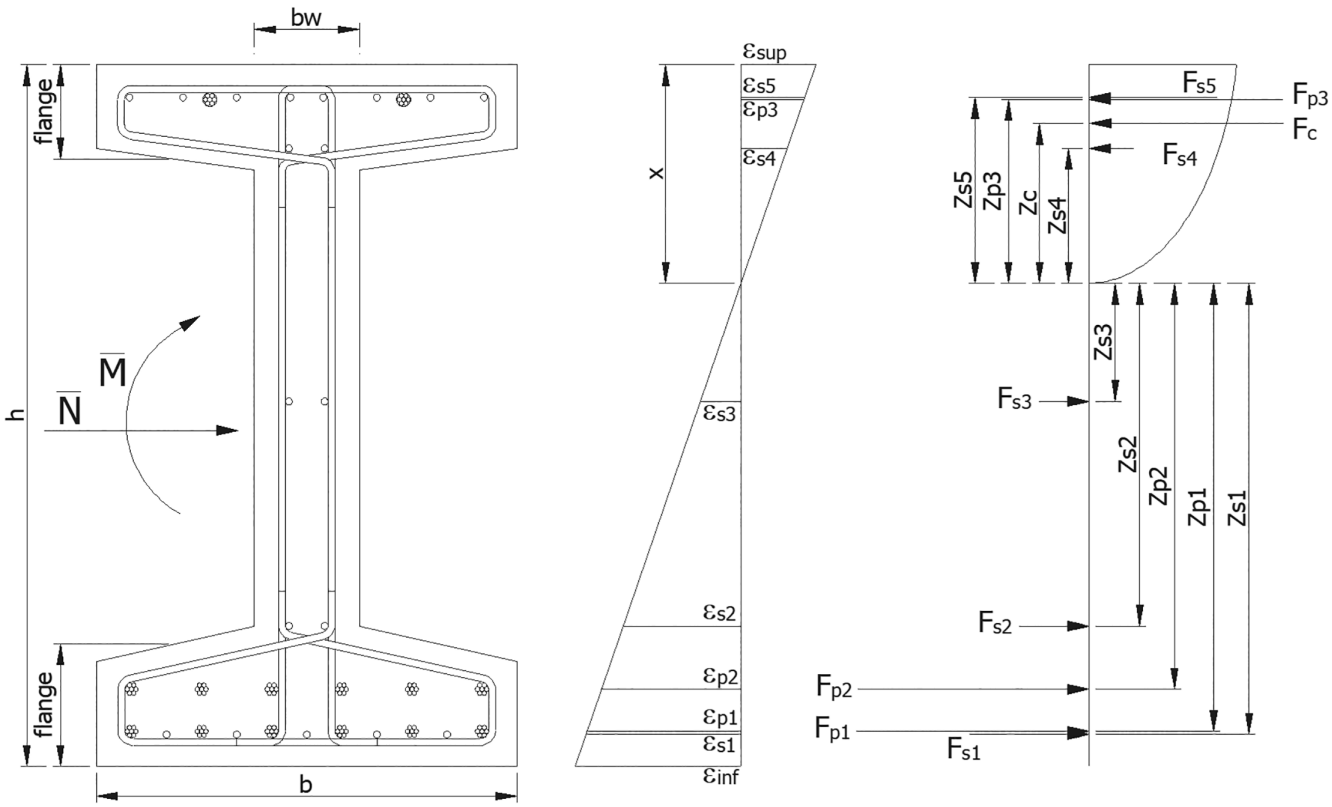

FIGURE 14 Adopted stress–strain diagram for the specimens "cross-sections"

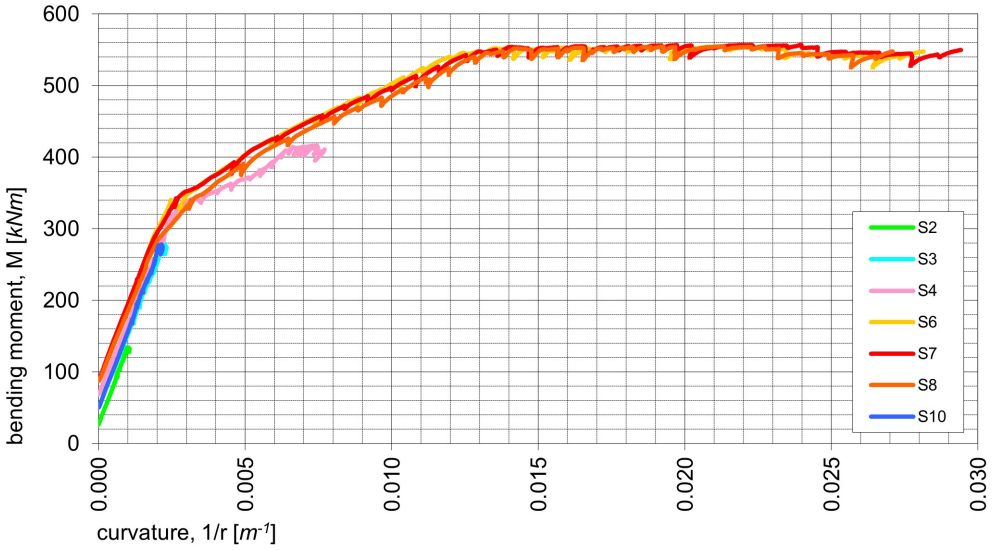

FIGURE 15 Moment-curvature diagrams of specimen V1

stress–strain law, can be reliably used to predict the flexural behavior of produced girders.

Figure 15 shows the bending moment-curvature diagrams obtained experimentally for specimen V1 at the monitored sections S2–S4, S6–S8, and S10. Very similar diagrams were obtained for specimen V2. The curvatures, 1/r, were evaluated by the ratio between the measurements provided by the strain gauges attached to the bottom and top reinforcing bars, and the distance between them (Figure 13). The bending moments were calculated based on the flexural effect of the applied force added to the girder's dead weight, the latter being the reason why plots in Figure 15 do not initiate at the origin. Diagrams corresponding to monitored sections S6, S7, and S8, those staying within the 6.0 m central length subjected to pure bending (see Figure 8), show, similarly to what has been observed in Figure 11, the three typical behavior stages (I–III) of a beam specimen subjected to bending. Plot respecting to section S4 remained in the crack spreading stage II and those related to sections S2, S3, and S10 did not overpass the linear elastic regimen. Figure 15 also shows very similar behavior between sections symmetrically positioned, that is, sections S3 and S10 and sections S6 and S8.

Figure 16 depicts a comparison between moment-curvature diagrams of specimens V1 and V2 at the mid-span section S7, and an analytical prediction. The latter was obtained by using the above-mentioned *Delphi* routine. A wide range of increasing strains at the top fiber were considered, and the corresponding bending moments were calculated. Strains were considered up to a maximum of −2.8‰, corresponding to the moment where concrete starts to crush. This defined the maximum bending moment and curvature of the cross section. Plots in Figure 16 show a sound agreement between experimental and analytical results within the complete curvature range, suggesting that the mechanical behavior of the hardened material, resulting from the mixture design published in,[14] is well described by the constitutive model recommended by Eurocode 2[13] and Model Code 2010.[19]

Figure 17 depicts the deformed shape of specimen V2 for increasing load steps, obtained based on the records provided by the displacement transducers placed at the monitored sections, and interpolating between these. A perfect match was observed with the results provided by the terrestrial photogrammetry. Initial precamber at mid-span section due to prestress measured 49.90 mm at the testing day, and each step identifier corresponds to the magnitude of the applied load. Thus, load steps 0 to 66, 75 to 120 and 125 to 142 respect to stage I (uncracked), stage II (crack spreading), and stage III (spread of yielding), respectively. Plots in Figure 17 confirm the ability of the specimen to undergo very significant deformations, up to structural failure. Very similar measurements were obtained for specimen V1, allowing to draw similar conclusions.

Figure 18 presents a comparison between deformed shapes of specimen V2 obtained experimentally and analytically, at the instant of cracking and structural failure. The analytical approaches were obtained by numerical integration of the average curvatures assessed between 19 different sections, spaced 1 m apart along the specimen length. A similar procedure to that performed to calculate the theoretical moment-curvature diagram presented in Figure 16 was replicated for the discretized sections. The average curvature between sections was calculated according to the weighting equation proposed in Eurocode 2[13] (see Equation [4]).

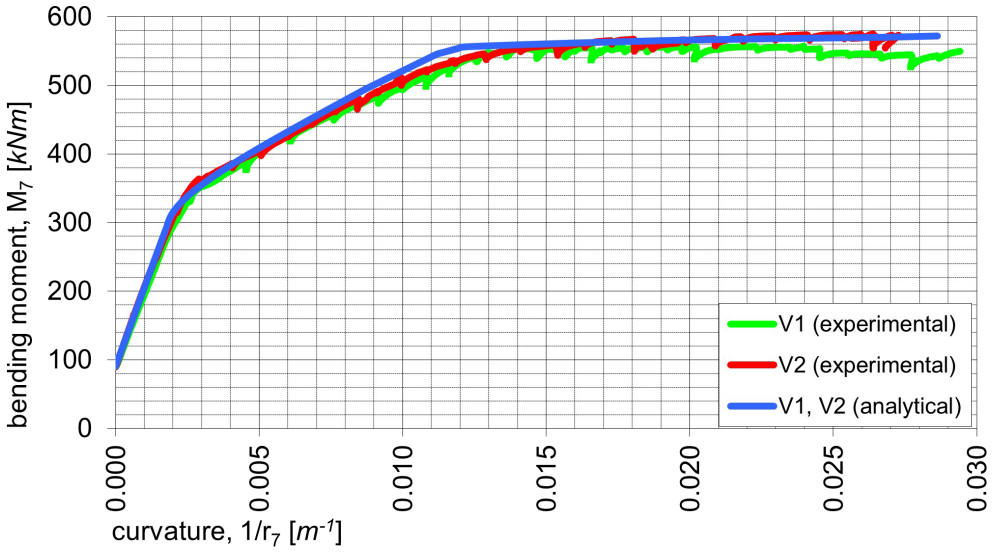

FIGURE 16 Analytical prediction of the moment/curvature diagram

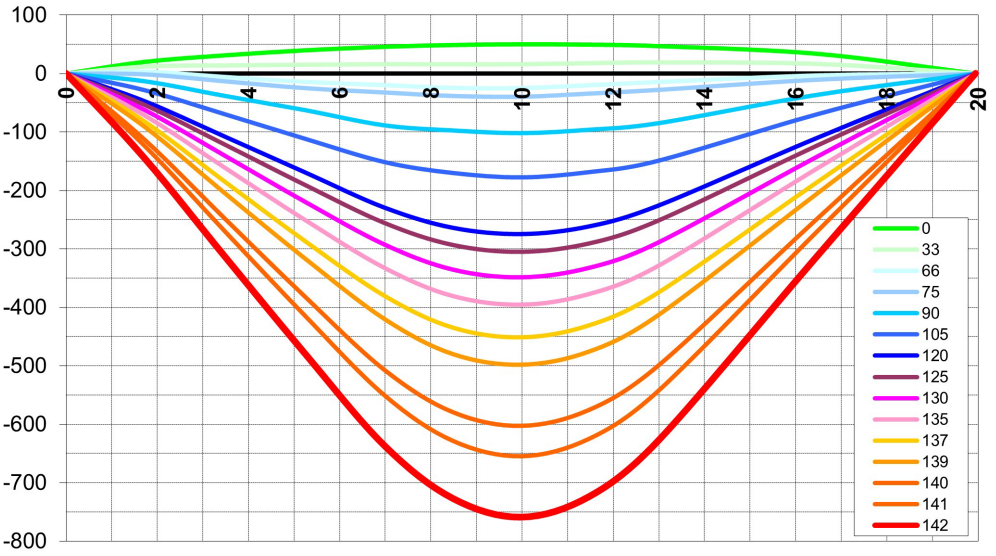

FIGURE 17 Deformed shape in mm of specimen V2 for increasing load steps

$$\frac{1}{r_m} = (1-\zeta)\frac{1}{r_I} + \zeta\frac{1}{r_{II}} \tag{4}$$

The distribution coefficient, ζ, was taken null for uncracked sections, or otherwise estimated based on Equation (5), suitable for the short-term loading of reinforced concrete[13] (see Figure 19):

$$\zeta = 1 - \left(\frac{M_{cr}}{M}\right)^2 \tag{5}$$

Neglecting the deflection related to the precamber, the displacements at the mid-span section, when girders V1 and V2 cracked for the first time, were 43.5 and 39.9 mm, respectively. Calculations estimated this same displacement in 41.9 mm, corresponding to relative differences of 3.7% and 5.0%. At the moment of structural failure, maximum displacements were 886.1 and 800.1 mm for specimens V1 and V2, respectively. The analytical approach resulted in 843.8 mm, thus presenting differences of 4.7% and 5.5%.

Comparison between experimental and analytical results show that both serviceability and ultimate deflections of the produced girders can be accurately predicted (relative error ranging from 3.7% to 5.5%) considering the methodology proposed in Eurocode 2.[13]

4 | CONCLUSIONS

The flexural behavior of slender (1/40) long-span (40 m) precast prestressed high-strength concrete girders was experimentally investigated regarding their use in highways' overpasses and as an economical alternative to steel girders,

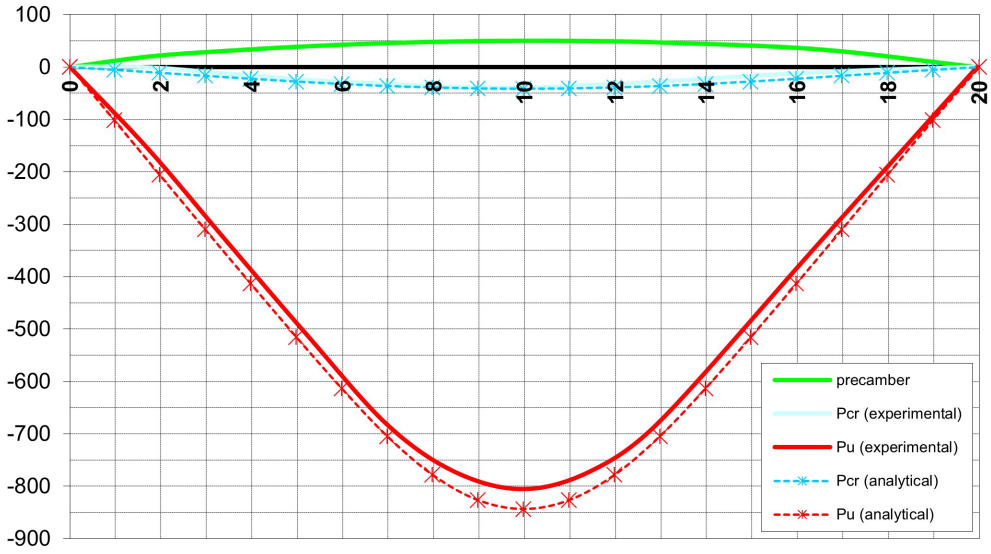

FIGURE 18 Comparison of the deformed shapes of specimen V2 obtained experimentally and analytically

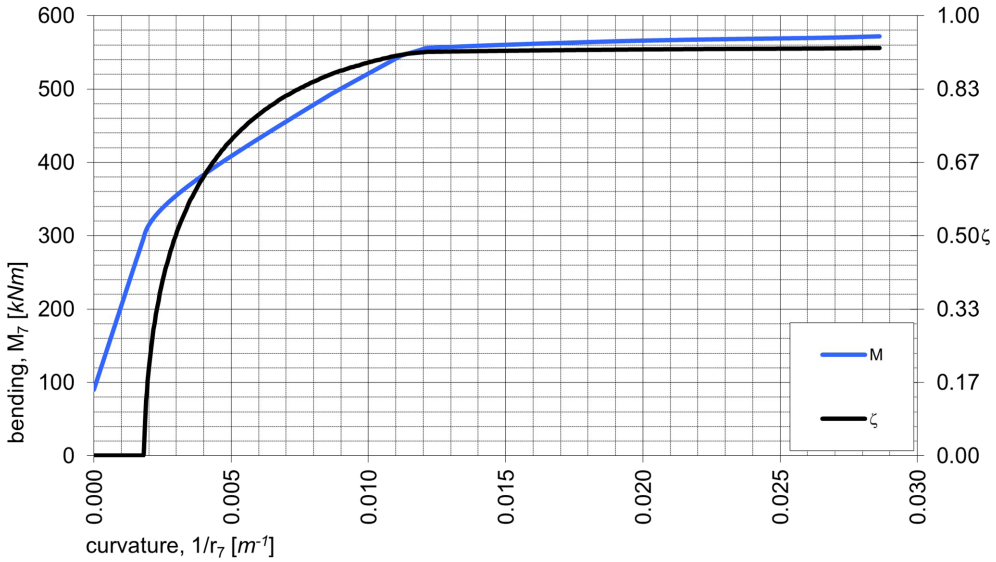

FIGURE 19 Calculation of the distribution coefficient ζ

the preferred structural solution for this purpose. Results of a free vibration test highlight the integrity of the tested specimens and indicate that damping is within the expected range for conventional prestressed uncracked concrete. Findings of the short-term loading indicate that slender long-span precast prestressed high-strength concrete girders exhibit the typical behavior of reinforced concrete members in bending, characterized by: (i) elastic behavior up to cracking; (ii) crack spreading stage; (iii) development of the failure mechanism. Although brittleness is usually related with high strength concrete, the experimental load–displacement and moment-curvature diagrams obtained show the ability of the tested specimens to experience large displacements with insignificant softening on the plastic regimen. The ratio between the displacements at failure and at yielding shows adequate ductility (2.6) of both specimens. An analytical approach, assuming plane sections and based on the short-term stress–strain relationship for concrete recommended by Eurocode 2,[13] was developed to predict the structural behavior of tested specimens under ultimate and serviceability conditions. Analytical predictions of cracking, yielding and maximum loads show a sound agreement with experimentally results. Estimates of deflections corresponding to cracking and failure of specimens matched experimental results with a 5% margin of error.

In view of the above, and based on the results of the short-term loading, it can be concluded that, despite the brittle behavior usually associated with non-fiber-reinforced high-strength concrete, long-span precast, and prestress concrete girders are suitable to be used for highway overpasses. However, further research is still needed, namely to characterize their long-term behavior, by assessing the time-dependent effects, not addressed in this paper.

ACKNOWLEDGMENTS

The authors would like to acknowledge all the support of Prégaia.

NOTATION

δ_i	displacement measured at section S_i
δ_y	displacement measured at section S_7 at yielding
δ_u	ultimate displacement measured at section S_7
$\varepsilon_{c(e,s,c)}$	global strain
ε_{ce}	elastic strain
ε_{cs}	Strain due to shrinkage
ε_{cc}	elastic due to creep
ε_{um}	mean value of reinforcing bars/prestressing strands ultimate strain
φ_c	creeping coefficient
ζ	distribution coefficient
f	frequency of vibration
f_{cm}	mean value of concrete compressive strength
f_{ym}	mean value of reinforcing bars/prestressing strands yielding stress
f_{um}	mean value of reinforcing bars/prestressing strands ultimate stress
t	time in days
$1/r$	mean curvature
$1/r_I$	curvature (uncracked section)
$1/r_{II}$	curvature (cracked section)
E_{cm}	mean value of concrete's Young's modulus
A_r	reinforcing bars/prestressing strands area
P	testing load
P_{cr}	cracking load
P_y	yielding load
P_u	maximum load
M_{cr}	cracking bending moment
M_y	yielding bending moment
M_u	maximum bending moment

DATA AVAILABILITY STATEMENT

The data that support the findings of this study are available from the corresponding author upon reasonable request.

ORCID

Paulo Fernandes https://orcid.org/0000-0002-5644-8889

Eduardo Cavaco https://orcid.org/0000-0001-6413-4217

REFERENCES

1. Maguire M, Morcous G, Tadros MK. Structural performance of precast/prestressed bridge double-tee girders made of high-strength concrete, welded wire reinforcement, and 18-mm-diameter strands. J Bridge Eng. 2013;18:1053–61. https://doi.org/10.1061/(asce)be.1943-5592.0000458
2. Villamizar S, Ramirez JA, Aguilar G. Shear strength and behavior of high-strength concrete prestressed beams. ACI Struct J. 2016;114:277–289. https://doi.org/10.14359/51689458
3. Yoo D-Y, Banthia N, Kang S-T, Yoon Y-S. Size effect in ultra-high-performance concrete beams. Eng Fract Mech. 2016;157:86–106. https://doi.org/10.1016/j.engfracmech.2016.02.009
4. Pansuk W, Nguyen TN, Sato Y, Den Uijl JA, Walraven JC. Shear capacity of high performance fiber reinforced concrete I-beams. Construct Build Mater. 2017;157:182–93. https://doi.org/10.1016/j.conbuildmat.2017.09.057
5. Shafieifar M, Farzad M, Azizinamini A. Experimental and numerical study on mechanical properties of ultra high performance concrete (UHPC). Construct Build Mater. 2017;156:402–11. https://doi.org/10.1016/j.conbuildmat.2017.08.170
6. Kodur V, Solhmirzaei R, Agrawal A, Aziz EM, Soroushian P. Analysis of flexural and shear resistance of ultra high performance fiber reinforced concrete beams without stirrups. Eng Struct. 2018;174:873–84. https://doi.org/10.1016/j.engstruct.2018.08.010
7. Dolan CW, Ballinger CA, LaFraugh RW. High strength prestressed concrete bridge girder performance. PCI J. 1993;38:88–97. https://doi.org/10.15554/pcij.05011993.88.97
8. Russell BW. Impact of high strength concrete on the design and construction of pretensioned girder bridges. PCI J. 1994;39:76–89.
9. Roller JJ, Martin BT, Russell HG, Bruce RN. Performance of prestressed high strength concrete bridge girders. PCI J. 1993;38:34–45.
10. Roller JJ, Russell HG, Bruce JRN, Martin BT. Long-term performance of prestressed, pretensioned high strength concrete bridge girders. PCI J. 1995;40:48–59. https://doi.org/10.15554/pcij.11011995.48.59
11. Hueste MBD. Flexural design of high strength concrete prestressed bridge girders-review of current practice and parametric study. Texas Transportation Institute, FHWA/TX-04/0–2101-3, 2003.
12. Russell, HG, Graybeal, BA. Ultra-high performance concrete: a state-of-the-art report for the bridge community. Federal Highway Administration (FHWA), FHWA-HRT-13-060, 2013.
13. CEN, *Eurocode 2: design of concrete structures: part 1: general rules and rules for buildings*. European Committee for Standardization, 1991.
14. Fernandes P, Pala H, Cavaco E, Tiago P, Júlio E. Admixture tuning for high-performance concrete for the production of novel precast pre-stressed long-span girders for highway overpasses. Struct Concr. 2020;21:1989–98. https://doi.org/10.1002/suco.201900090
15. European Committee for Standardization, *EN 206-1: concrete. Specification, performance, production and conformity*. 2000.
16. European Committee for Standardization, *EN 12390-3: testing hardened concrete. Compressive strength of test specimens*. 2009.
17. European Committee for Standardization, *EN 10080: steel for the reinforcement of concrete. Weldable reinforcing steel. General*. 2009.
18. Bachmann H, Ammann WJ, Deischl F, Eisenmann J, Floegl I, Hirsch GH, et al. Vibration problems in structures: practical guidelines. Switzerland: Birkhäuser; 2012.
19. FIB. Fib model code for concrete structures 2010. Lausanne: Ernst & Sohn, Wiley; 2013.

AUTHOR BIOGRAPHIES

Paulo Maranha
Instituto Superior de Engenharia de Coimbra
Instituto Politécnico de Coimbra
Coimbra, Portugal
Email: pmtiag@vodafone.pt

Eduardo Júlio
Instituto Superior Técnico
Universidade de Lisboa
Lisboa, Portugal
Email: eduardo.julio@tecnico.ulisboa.pt

Paulo Fernandes
Instituto Politécnico de Leiria
Leiria, Portugal
Email: paulo.fernandes@ipleiria.pt

Eduardo Cavaco
Faculdade de Ciências e Tecnologia
Universidade NOVA de Lisboa
Lisboa, Portugal
Email: e.cavaco@fct.unl.pt

How to cite this article: Fernandes P, Cavaco E, Maranha P, Júlio E. Flexural behavior of slender long-span precast prestressed high-strength concrete girders. Structural Concrete. 2021;22: 2272–2288. https://doi.org/10.1002/suco.202100070